Structural and Functional Characterization of the Phosphorylated Adipocyte Lipid-Binding Protein (pp15)†

Melissa K. Buelt,‡ Zhaohui Xu,§ Leonard J. Banaszak,§ and David A. Bernlohr*,‡

Department of Biochemistry, College of Biological Sciences, University of Minnesota, St. Paul, Minnesota 55108, and Department of Biochemistry, School of Medicine, University of Minnesota, Minneapolis, Minnesota 55455

Received August 6, 1991; Revised Manuscript Received December 27, 1991

ABSTRACT: A substrate for the insulin receptor kinase in 3T3-L1 adipocytes has previously been identified as the adipocyte lipid-binding protein (ALBP, also known as aP2 or p15). We have characterized the effect of tyrosyl phosphorylation on ALBP structure and ligand-binding properties. Phosphorylated ALBP (phospho-ALBP) was isolated by a combination of gel filtration, anion exchange chromatography, and immunoaffinity chromatography on anti-phosphotyrosine agarose. Circular dichroic spectroscopy indicated that the phosphoprotein was similar in structure to native ALBP. Phospho-ALBP exhibited a slight decrease in calculated α-helical content which was compensated for by an increase in β-sheet structure. The wavelength yielding maximum tryptophan fluorescence was unaltered by phosphorylation (334 ± 1 nm). However, the concentration of guanidine HCl yielding 50% denaturation was 1.43 M for ALBP and 0.92 M for phospho-ALBP. The $\Delta G°_{app}$ was 3.87 and 3.25 kcal mol^{-1} for ALBP and phospho-ALBP, respectively, suggesting that phosphorylation destabilized the protein. To assess the binding characteristics of the phosphoprotein, a long-chain fatty acid affinity column was synthesized to which native ALBP specifically bound. In contrast, phospho-ALBP showed little or no affinity for the column. Furthermore, phosphorylation virtually abolished binding of the fluorescent fatty acid analogue 12-(9-anthroyloxy)oleic acid. Fatty acid binding activity was recovered (~60%) upon dephosphorylation with protein tyrosine phosphatase. The structural studies, coupled with the crystal structure of the apoprotein, indicate that the dramatic reduction in binding affinity is likely a result of steric hindrance in the binding cavity or of electrostatic interactions of the phosphoryl group with the fatty acid. The present study reveals that phosphorylation blocks ligand binding and suggests that an insulin-regulated phosphorylation/dephosphorylation cycle may be utilized for directionally orienting lipid flux in adipocytes.

One of the primary targets of insulin action is adipose tissue. Insulin acts via interaction with its heterotetrameric plasma membrane receptor, which, upon binding of hormone, undergoes self-catalyzed phosphorylation on its cytoplasmic β-subunit. Autophosphorylation activates the tyrosine kinase activity of the receptor (Rosen, 1987). A large body of evidence suggests that tyrosine phosphorylation is essential for the majority of insulin's effects (Ellis et al., 1986; Morgan & Roth, 1987). In the adipocyte, the association of insulin with the receptor results in an increase in the activities of enzymes involved in energy storage processes such as glucose and fatty acid uptake and lipogenesis. Coincident with the activation of lipogenesis there occurs a decrease in lipolysis via dephosphorylation of hormone sensitive lipase.

The flux of fatty acids in lipid metabolizing tissues appears to be mediated by fatty acid binding proteins, members of a family of intracellular low molecular weight proteins which stoichiometrically and saturably bind hydrophobic ligands [for reviews, see Matarese et al. (1990) and Sweetser et al. (1987)]. The adipocyte constituent of the family is the adipocyte lipid-binding protein (ALBP),[1] also termed 422 protein, aP2, and p15 (Bernlohr et al., 1985; Hunt et al., 1986; Hresko et al., 1988). ALBP has been isolated from a number of sources such as murine 3T3-L1 cells (Matarese & Bernlohr, 1988) and human and porcine adipose tissue (Baxa et al., 1989; Armstrong et al., 1990), and its in vitro binding properties have been well characterized (Buelt & Bernlohr, 1990; Matarese & Bernlohr, 1988; Wootan et al., 1990). Furthermore, previous studies by our laboratory provided the first convincing in situ evidence that a fatty acid binding protein is involved in lipid uptake and transport (Waggoner & Bernlohr, 1990).

In addition to its fatty acid binding activity, it has recently been shown that ALBP is a substrate for the insulin receptor kinase in 3T3-L1 cells treated with insulin and phenylarsine oxide (Bernier et al., 1987; Hresko et al., 1988). The phosphorylation was subsequently characterized in vitro with a reconstituted system using WGA-Sepharose eluate containing insulin receptor from 3T3-L1 cells and homogeneous ALBP (Chinander et al., 1989; Hresko et al., 1990). Utilizing the soluble kinase domain of the insulin receptor β-subunit (Cobb et al., 1989; Herrera et al., 1988) to eliminate detergent–fatty acid interactions, we have previously demonstrated that the presence of a bound lipid increased the k_{cat}/K_m relative to that of the apoprotein (Buelt et al., 1991). Having demonstrated that fatty acid binding activates phosphorylation, the purpose of the present study was to determine whether phosphorylation influences the structural characteristics and lipid-binding properties of ALBP. We report here that phosphorylation blocks ligand binding without a dramatic effect on overall

† This work was supported by NSF Presidential Young Investigator Award DMB8552942 to D.A.B. and by NIH Grant GM13925 to L.J.B.

* Author to whom correspondence should be addressed, at the Department of Biochemistry, University of Minnesota, 1479 Gortner Ave., St. Paul, MN 55108.

‡ College of Biological Sciences.

§ School of Medicine.

[1] Abbreviations: ALBP, adipocyte lipid-binding protein; IFABP, intestinal fatty acid binding protein; LFABP, liver fatty acid binding protein; CD, circular dichroism; PAO, phenylarsine oxide; pNPP, *p*-nitrophenyl phosphate; phospho-ALBP, phosphorylated ALBP; 12-AO, 12-(9-anthroyloxy)oleic acid; GdnHCl, guanidine hydrochloride; IR, insulin receptor; WGA, wheat germ agglutinin; DTNB, 5,5′-dithiobis(2-nitrobenzoic acid); PTPase, protein tyrosine phosphatase.

0006-2960/92/0431-3493$03.00/0

protein organization and analyze this data in reference to the crystal structure of apo-ALBP.

Experimental Procedures

Materials. [γ-^{32}P]ATP (3000 Ci/mmol) was purchased from Amersham. Oleic acid was obtained from NuChek Prep, Inc. (Elysian, MN), 12-aminolauric acid was from Fluka, and 12-(9-anthroyloxy)oleic acid was from Molecular Probes. The anti-phosphotyrosine agarose was purchased from Oncogene Science, and the insulin was obtained from GIBCO. The WGA-Sepharose, 6-aminohexanoic acid-activated Sepharose 4B, DEAE-Sephadex, *p*-nitrophenyl phosphate, and DTNB were from Sigma. Guanidine HCl was from Bethesda Research Laboratories. All other materials were reagent grade.

Protein Preparation. ALBP was purified from cultured murine 3T3-L1 adipocytes essentially as described by Matarese and Bernlohr (1988) or from expressing *Escherichia coli* (Xu et al., 1991). Protein concentration was determined using an extinction coefficient at 280 nm of 1.55×10^4 M^{-1} cm^{-1}. The 3T3-L1 insulin receptor was partially purified from confluent adipocyte monolayers using a modified procedure of Kohanski and Lane (1983) as previously described (Chinander & Bernlohr, 1989).

Phospho-ALBP was prepared using either the 3T3-L1 partially purified holoreceptor or the soluble kinase domain of the receptor (Cobb et al., 1989; Herrera et al., 1988). ALBP was phosphorylated with WGA-Sepharose eluate containing IR (Chinander & Bernlohr, 1989). In brief, holoreceptor was autophosphorylated in 25 mM Tris-HCl, pH 7.4, 10 mM $MgCl_2$, 4 mM $MnCl_2$, 100 μM [^{32}P]ATP, and 100 nM insulin for 60 min at ambient temperature. Substrate phosphorylation was then initiated by the addition of ALBP (typically 1–2 mg) in Tris buffer containing metals and ATP. Phosphorylation using the soluble kinase was as described previously (Buelt et al., 1991). Kinase was autophosphorylated in 25 mM Tris-HCl, pH 7.4, 5 mM $MnCl_2$, and 250 μM [^{32}P]ATP for 60 min at ambient temperature after which time ALBP was added. Because the rate of phosphorylation was relatively slow, long term phosphorylations (24–48 h) were carried out to maximize the yield of phosphoprotein. In typical phosphorylation reactions, 10% of ALBP was converted to its phosphorylated form. ATP was removed by passing the reaction mixture through an Excellulose GF-5 desalting column (Pierce) equilibrated in 25 mM Tris-HCl, pH 7.4. The yield of phospho-ALBP recovery from the desalting column was generally greater than 90% as judged by SDS–PAGE followed by autoradiography. Protein-containing fractions were pooled and applied to DEAE-Sephadex in the same buffer. ALBP and phospho-ALBP were quantitatively recovered in the nonbinding fractions, while phosphorylated insulin receptor and ATP bound tightly. The protein mixture was then applied to the anti-phosphotyrosine agarose column equilibrated in 25 mM Tris-HCl, pH 7.4, and eluted with 10 mM *p*-nitrophenyl phosphate in the same buffer. As judged by SDS–PAGE and autoradiography, 75% of the phospho-ALBP was recovered in the pNPP elution, and the remainder was tightly associated with the resin. The pNPP was subsequently removed by repetitive dilution and concentration in a Centricon 10 microconcentrator (Amicon). Typically 100–150 μg of phospho-ALBP could be isolated by these procedures.

To verify that the phospho-ALBP was homogeneous and that nonphosphorylated material did not copurify, two determinations were made. Firstly, the molar amount of phospho-ALBP determined by spectrophotometry agreed to within 10% of that determined by radioisotopic determination. If significant amounts of nonphosphorylated ALBP had copurified, then the amount of protein determined spectroscopically would have exceeded that determined by radioactivity. In this determination we are assuming that the extinction coefficient of phospho-ALBP is not significantly different from that of ALBP. This is likely to be a valid assumption for ALBP besides having two tyrosine residues contains two tryptophan residues which dominate the absorption spectrum. A second independent method was also utilized to verify the purity of phospho-ALBP. Native ALBP is a basic protein with an isoelectric point of 9.1, while phospho-ALBP has a drastically altered value of 5.8 (Hresko et al., 1988; Matarese & Bernlohr, 1988). When analytical isoelectric focusing was performed (Pharmacia PhastGel; pH range 3–10), all of the protein migrated at the acidic value and was coincident with the radioactivity determined by autoradiography. The absence of ALBP at the basic range of the gel indicated that the preparations were devoid of contaminating nonphosphorylated material.

Circular Dichroic Analysis. The CD spectra were measured at ambient temperature with a Jasco J-41C spectropolarimeter calibrated with d_{10}-camphorsulfonic acid. Spectra for ALBP (2.7 μM) and for phospho-ALBP (2.1 μM) in 25 mM Tris-HCl, pH 7.4, were recorded from 260 to 195 nm at 10 nm/min using a cell path length of 0.1 cm. Four scans were recorded, averaged, and expressed in terms of mean residue ellipticity. Data were analyzed using a least-squares fitting program based on the reference spectra reported by Chang et al. (1978) or by the formalism described by Nagy and Strzelecka-Golaszewska (1972).

Protein Denaturation. Equilibrium unfolding as a function of denaturant concentration was monitored by fluorescence spectroscopy in the presence of guanidine HCl. Emission spectra of 0.5 μM ALBP or phospho-ALBP in 25 mM Tris-HCl, pH 7.4, containing increasing concentrations of GdnHCl were recorded at 25 °C with a Perkin-Elmer 650-10S fluorescence spectrophotometer using an excitation wavelength of 285 nm with 4-nm slits. The emission wavelength yielding maximum fluorescence was plotted vs denaturant concentration for each sample to visualize the unfolding profile. The Gibbs free energy, ΔG, was calculated for each data point according to $\Delta G = -RT \ln K$ and was replotted vs denaturant concentration. Line fitting by linear regression was used to determine $\Delta G°_{app}$, the free energy difference between the folded and unfolded forms of the protein linearly extrapolated to zero GdnHCl concentration, and C_m, the concentration of denaturant at the midpoint of the transition (Shortle, 1989).

Synthesis of Long-Chain Fatty Acid Affinity Column. A long-chain fatty acid affinity column was synthesized by coupling 12-aminolauric acid (Fluka) to *N*-hydroxysuccinimide esterified hexanoic acid–Sepharose 4B (Sigma). The 12-aminolauric acid (5 mM) was dissolved at 65 °C in 10 mL of 100 mM $NaHCO_3$, pH 8, and 0.5 M NaCl. The ligand was then mixed with 0.5 g of washed resin and incubated for 2 h at 37 °C with gentle rotation. Following coupling, the unreacted resin was modified with 1 M ethanolamine for 1 h at ambient temperature. Unreacted 12-aminolaurate was then removed with successive washes in high pH (50 mM Tris-HCl, pH 8, 0.5 M NaCl) and low pH (50 mM sodium acetate, pH 4, 0.5 M NaCl) buffers. The ALBP-binding capacity was determined to be approximately 100 μg/mL of resin.

Fatty Acid Binding. Ligand binding was assessed by applying protein to the fatty acid affinity column equilibrated in 25 mM Hepes, pH 7.5. The column was washed with the same buffer, and protein was eluted with 1 M NaCl in 25 mM

Hepes, pH 7.5. The elution profile was followed spectroscopically and, for phospho-ALBP, by radioactivity.

Fatty acid affinity was also assessed using the fluorescent fatty acid analogue 12-(9-anthroyloxy)oleic acid. 12-AO was quantitated using $\epsilon_{383} = 6400\ M^{-1}\ cm^{-1}$ in absolute ethanol and diluted into buffer with mixing for use. The concentration of 12-AO remained constant at 50 nM, while ALBP ranged from 0 to 7.5 μM in 25 mM Tris-HCl, pH 7.4, in a 300-μL reaction volume. Fluorescence of the probe was measured with an excitation wavelength of 383 nm and an emission wavelength of 460 nm. All manipulations were done in dim light. To assess whether dephosphorylation of phospho-ALBP would restore binding activity, the phosphoryl group was first removed by incubation with 5 μg of the rat brain PTPase denoted GST-PTPU323 (Guan et al., 1990; Guan & Dixon, 1991) for 30 min at 37 °C in 50 mM sodium acetate, pH 6. The reaction mixture was diluted into binding buffer, and unphosphorylated ALBP was isolated by passing through a Centricon 30 microconcentrator (Amicon). GST-PTPU323, a glutathione-*S*-transferase fusion protein with a molecular mass of ~63 kDa, remained in the retentate. Complete dephosphorylation was verifed by SDS–PAGE and autoradiography. ALBP was handled similarly as a control to ensure the procedure had no effect on binding.

Results

ALBP is a fatty acid binding protein shown to be phosphorylated on Tyr^{19} by the insulin receptor in 3T3-L1 adipocytes. We (Buelt et al., 1991) and others (Hresko et al., 1990) have previously shown that ligand binding increases the phosphorylation potential of ALBP by decreasing the K_m 10-fold, suggesting that insulin-stimulated phosphorylation may modulate the role of the binding protein in lipid trafficking and metabolism. The present study was undertaken to characterize the effect of phosphorylation on ALBP structure and function.

To examine the structure of the phosphoprotein, it was first necessary to isolate homogeneous phospho-ALBP by a series of steps concluding with immunoaffinity chromatography. After phosphorylation, the reaction mixture was subjected to gel filtration and anion exchange chromatography to remove unreacted ATP and receptor kinase. Both ALBP and its phosphorylated counterpart were found in the nonbinding fractions from DEAE-Sephadex at pH 7.4. When the ALBP-containing fractions were pooled and applied to antiphosphotyrosine agarose, the phosphoprotein quantitatively bound to the column, indicating that the phosphotyrosyl group was accessible for recognition by the monoclonal antibody (results not shown).

Structural Analysis of Phospho-ALBP. To determine the effects of phosphorylation on protein structure, circular dichroic spectroscopy of ALBP was conducted (Figure 1). For native ALBP, the CD spectrum was characterized as a broad trough with a wavelength minimum of 215 nm. The spectrum for phospho-ALBP followed the same general pattern, with a narrower trough and a shift in the minimum ellipticity signal to 217 nm. The value of $[\theta]_{222}$ for ALBP was −5750 deg cm^2 dmol^{-1}, corresponding to 15% α-helical structure if 100% helix structure has a value of −38 500 at 222 nm (Nagy & Strzelecka-Golaszewska, 1972) or if the data are analyzed by fitting the whole spectrum with a least-squares procedure using the reference spectra of Chang et al. (1978). The latter analysis predicted that ALBP is composed of about 61% β-sheet. Taken together these data correlated well with the secondary structure determined by the method of Kabsch and Sander (1983) from the crystal structure of apo-ALBP (58% β-sheet and 13% α-helix; Xu et al., 1992). The phosphoprotein exhibited a reduction in the α-helix content to 9% according to the algorithm described by Chang et al. (1978). On the basis of the computer analysis, this decrease in helical content was compensated for by an increase in the β-sheet structure, rather than by an increase in random coil. The CD indicated that, although a slight conformational change occurred upon phosphorylation, the protein was not grossly altered by the modification under the conditions utilized nor was the phosphoprotein a denatured molecule.

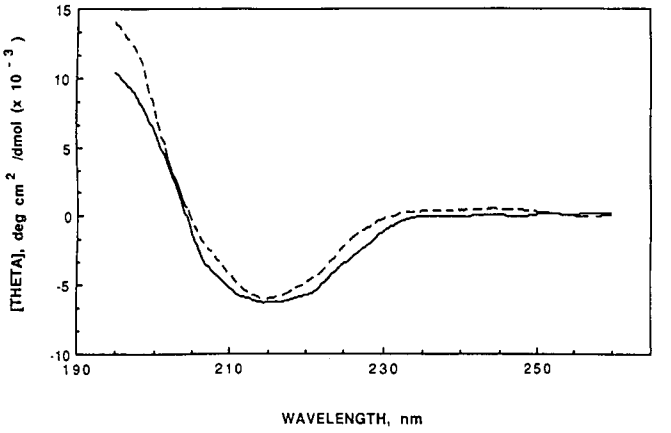

FIGURE 1: Circular dichroic spectra of ALBP and phospho-ALBP. CD spectra of 2.7 μM ALBP (solid line) and 2.1 μM phospho-ALBP (dashed line) in 25 mM Tris-HCl, pH 7.4 were measured at ambient temperature. Spectra represent the average of four scans expressed in terms of mean residue ellipticity in units of deg cm^2 dmol^{-1}.

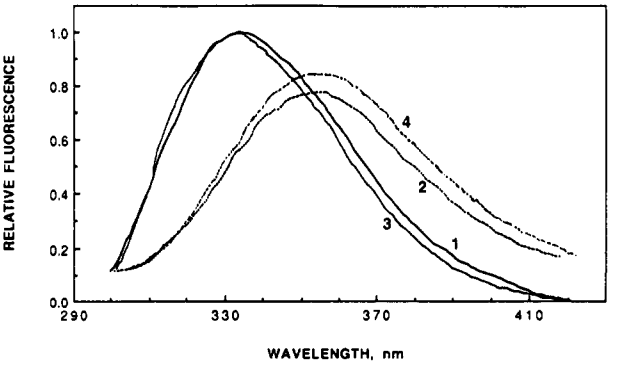

FIGURE 2: Intrinsic tryptophan fluorescence of ALBP and phospho-ALBP. Emission spectra of ALBP (lines 1 and 2) and of phospho-ALBP (lines 3 and 4) were recorded at 25 °C at a protein concentration of 0.5 μM in 25 mM Tris-HCl, pH 7.4. The excitation wavelength was 285 nm. Maximum emission occurred at 334 nm for both proteins as shown from lines 1 and 3. Fluorescence spectra in the presence of 3 M GdnHCl are shown in lines 2 and 4. The maximum emission was shifted to 355 nm for both unmodified and phospho-ALBP. Spectra are given for one trial representative of at least three experiments.

The integrity of the structure of phospho-ALBP was further evaluated by examination of the fluorescence spectrum of the protein. ALBP fluorescence arises primarily from two tryptophans, Trp^8 and Trp^{97}. From crystallographic analysis of apo-ALBP, Trp^8 lies internally on β-strand A, while Trp^{97} resides on strand G, near the reverse turn between strands G and H (Xu et al., 1992). ALBP and phospho-ALBP yield nearly identical spectra with a λ_{max} of 334 nm when excited at 285 nm, suggesting that the tryptophan residues reside in similar environments in both proteins (Figure 2). We examined the relative stability of the proteins by determining ΔG°_{app}, the free energy change in the absence of denaturant. Complete denaturation of ALBP with GdnHCl resulted in a red-shift of the emission maximum to 355 nm. This was

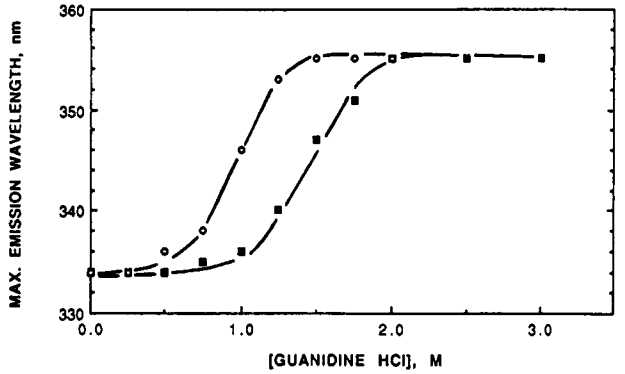

FIGURE 3: Guanidine HCl denaturation of ALBP and phospho-ALBP. Fluoresence emission spectra of ALBP and phospho-ALBP were recorded in the presence of increasing concentrations of GdnHCl. All spectra were recorded at 25 °C at an excitation wavelength of 285 nm. The wavelength yielding maximum emission fluoresence was plotted vs denaturant concentration for ALBP (■) and for phospho-ALBP (○). Linear extrapolations to zero GdnHCl concentration gave $\Delta G°_{app}$ of 3.87 kcal mol^{-1} for ALBP and 3.25 kcal mol^{-1} for phospho-ALBP. The midpoint of the transition occurred at 1.43 and 0.92 M GdnHCl for ALBP and for phospho-ALBP, respectively.

accompanied by a reduction in quantum yield as evidenced by a decrease in intrinsic tryptophan fluorescence. This phenomenon is similarly observed for phospho-ALBP.

The transition profiles for denaturation are shown in Figure 3. The curves follow similar patterns, though the midpoint of the transition for phospho-ALBP occurred at a much lower GdnHCl concentration. The $\Delta G°_{app}$ for ALBP was 3.87 kcal mol^{-1} with a midpoint of transition, C_m, at 1.43 M GdnHCl. Phosphorylation decreased the stability of the protein, exhibiting a $\Delta G°_{app}$ of 3.25 kcal mol^{-1} and a C_m of 0.92 M. This value for ALBP is lower than that reported for the related family member IFABP using GdnHCl as the denaturant as assessed by fluorescence tryptophan emission ($\Delta G°_{app}$ = 5.2 kcal mol^{-1}; Ropson et al., 1990). The denaturation process was reversible, as evidenced by a return of the maximum emission wavelength to 334 nm upon dilution of GdnHCl (data not shown). That phospho-ALBP is less stable than its unmodified precursor is intriguing; it will be of interest to determine whether other tyrosyl phosphorylated proteins exhibit similar changes in stability.

Ligand-Binding Affinity of Phospho-ALBP. Phospho-ALBP was determined to be structurally competent by CD and fluorescence analysis. To examine the effect of phosphorylation on ligand binding, a long-chain fatty acid affinity column was designed having the unique feature of a free carboxylate group at the terminus for coordination with arginine residues within the binding domain. Previous studies from this laboratory (Matarese & Bernlohr, 1988) have demonstrated that ALBP will not associate with a short-chain fatty acid affinity matrix (C_6) with a free carboxylate or with carboxymethyl-Sephadex resins, indicating that the association of ALBP with the column is not via an ion-exchange interaction but by virtue of its long-chain character. Moreover, ALBP does not bind to an aliphatic C_{18} resin, indicating that the hydrophobic nature of the synthesized resin is not nonspecifically associating with the lipid-binding protein. It has previously been shown from the IFABP and P2 crystal structures that the guanidinium groups of arginine residues buried in the β-clam of the proteins are involved in a hydrogen-bonding network with the carboxylate group of the bound fatty acid (Sacchettini et al., 1989a,b; Jones et al., 1988). Crystallographic analysis of ALBP (Xu et al., 1992) revealed that Arg^{106} and Arg^{126} are oriented internally, within the putative binding cavity. Furthermore, chemical modification

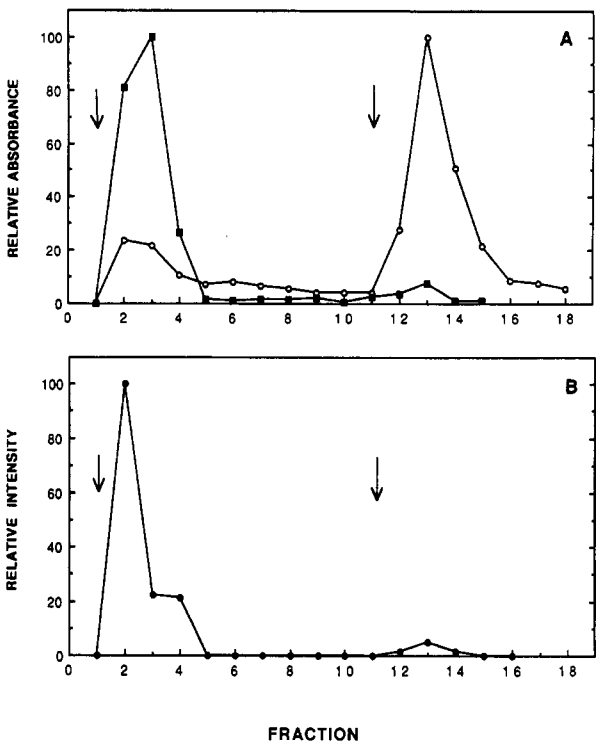

FIGURE 4: Fatty acid affinity column elution profiles. A long-chain affinity column was synthesized which terminated in a free carboxylate group. Various forms of ALBP were applied to the fatty acid affinity column (first arrow), washed, and eluted with 1 M NaCl in wash buffer (second arrow). The elution profiles were determined spectroscopically and, for phospho-ALBP, by radioactivity. (A) ALBP (○); DTNB-modified ALBP (■); (B) phospho-ALBP (●).

of arginine residues of ALBP significantly reduced binding affinity (Buelt & Bernlohr, 1990), such that these residues presumably interact with the carboxylate group of the bound lipid as observed for the aforementioned family members. Consequently, only long-chain resins with a free carboxylate contain the two components necessary for binding. The length of the affinity ligand is hypothesized to allow the fatty acid to extend from the site of ligand entry into the protein to Arg^{126} for ionic interaction. Alteration of either component by either shortening the aliphatic chain length or by eliminating the carboxylate negates binding.

To determine the specificity of the fatty acid affinity column, various modified forms of ALBP were applied to the column, and the elution profiles are shown in Figure 4. ALBP readily bound to the column and eluted with high salt. In contrast, ALBP modified on Cys^{117} with DTNB showed little affinity for the lipid (Figure 4A). Cys^{117} lies within the binding domain, and such modification has previously been shown to sterically block ligand binding (Buelt & Bernlohr, 1990). If ALBP was associating with the affinity matrix at a site on the protein other than the binding domain, the modification of internally oriented Cys^{117} would not influence binding. Furthermore, LFABP does not bind to the column (data not shown). ^{13}C NMR studies indicate that the carboxylate groups of fatty acids which are bound to this protein are solvent accessible and titrate with a normal pK_a (Cistola et al., 1988). The column was therefore concluded to be a specific and effective method for addressing ligand binding. When phospho-ALBP was applied to the column, very little bound, and virtually all of the radiolabeled protein was detected in the flow-through fractions (Figure 4B). This result demonstrated that the phosphorylated form of ALBP was essentially devoid of binding activity.

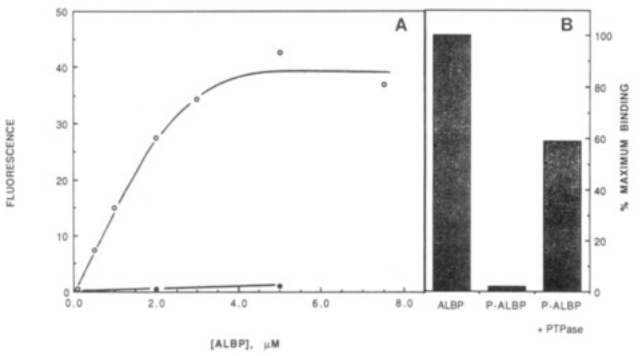

FIGURE 5: 12-(9-Anthroyloxy)oleic acid binding of ALBP and phospho-ALBP. (A) 50 nM 12-AO in 25 mM Tris-HCl, pH 7.4, was titrated with 0–7.5 μM ALBP (○) or with 0–5 μM phospho-ALBP (●). The change in fluorescence was measured at 25 °C with an excitation wavelength of 383 nm and an emission wavelength of 460 nm. (B) Phospho-ALBP was dephosphorylated with PTPase for 30 min at 37 °C. The PTPase was removed and 12-AO binding of ALBP was assayed at 0.74 μM. Results are reported as percent of maximum binding observed at the protein concentration and represent data from one trial of three experiments.

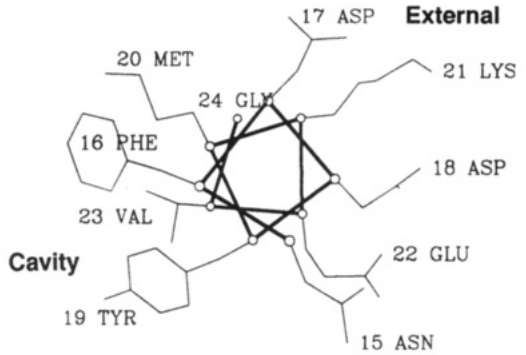

FIGURE 6: Phosphorylation site of ALBP on helix αI. Helix αI (Phe^{16}–Val^{23}) and two terminal residues (Asn^{15} and Gly^{24}) are shown. The backbone is represented by a α-carbon model. The view is along the helix axis with the backbone running away from the reader. The bold labels indicate the environment of the side chains; "external" refers to that portion of the helix which is accessible to the receptor kinase and "cavity" to that which lies adjacent to the fatty acid binding domain.

The affinity of phospho-ALBP for fatty acids was also assessed in a fluorescence binding assay utilizing the oleic acid derivative 12-AO. This ligand increases in fluorescence when bound within the binding domain (Storch et al., 1989). Native ALBP binds with high affinity, with a K_d of ~1 μM by Scatchard analysis (Figure 5A). In contrast, phospho-ALBP exhibits a dramatically reduced affinity ($K_d \gg 50$ μM). To indicate that the binding domain is not irreversibly disrupted upon phosphorylation, the phosphoryl group was removed by incubation with protein tyrosyl phosphatase and assayed for 12-AO binding; results are shown in Figure 5B. Upon PTPase treatment of the phosphoprotein, about 60% of the binding activity was recovered. Because the integrity of the protein is retained upon phosphorylation and its binding activity is restored with dephosphorylation, the lack of binding is likely the result of an electrostatic or steric hindrance to lipid association. However, we cannot eliminate the possibility of undetected local conformational effects.

Discussion

The search for physiologically relevant insulin receptor substrates has revealed several candidate proteins including p185 (White et al., 1985), microtubule associated protein-2 kinase (Ray & Sturgill, 1988), and phosphatidylinositol-3-kinase (Ruderman et al., 1990; Endemann et al., 1990). ALBP was first demonstrated to be phosphorylated in 3T3-L1 cells treated with PAO and insulin by Hresko et al. (1988). The phosphorylated residue, Tyr^{19}, resides on helix αI preceded by several acidic residues (Matarese & Bernlohr, 1988), analogous to the tyrosine kinase substrate consensus sequence (Cooper et al., 1984). The acidic residues of the helix are externally oriented and are thereby available for recognition by the receptor kinase (Figure 6). On the basis of a number of model peptide studies, it is clear that the acidic cluster near the site of phosphorylation is essential (White & Kahn, 1986). Although there exists some limited sequence similarity in the ALBP amino acid sequence 104–124 to published SH2 domain sequences (Sadowski et al., 1986; Koch et al., 1991; M.K.B. and D.A.B., unpublished observation), the primary kinase recognition motif would appear to be the acidic domain surrounding Tyr^{19}.

In contrast to the accessible acidic residues, the crystal structure of apo-ALBP has revealed that the phosphorylation site is buried (Figure 7). Tyr^{19} points into the ligand binding cavity of ALBP, as do the corresponding residues of myelin P2 and in IFABP (Jones et al., 1988; Sacchettini et al., 1989a). Recently, Buelt et al. (1991) have reported the in vitro phosphorylation properties of ALBP by the insulin receptor. As noted in that study, the velocity of phosphorylation was relatively slow. From an analysis of the structure of apo-

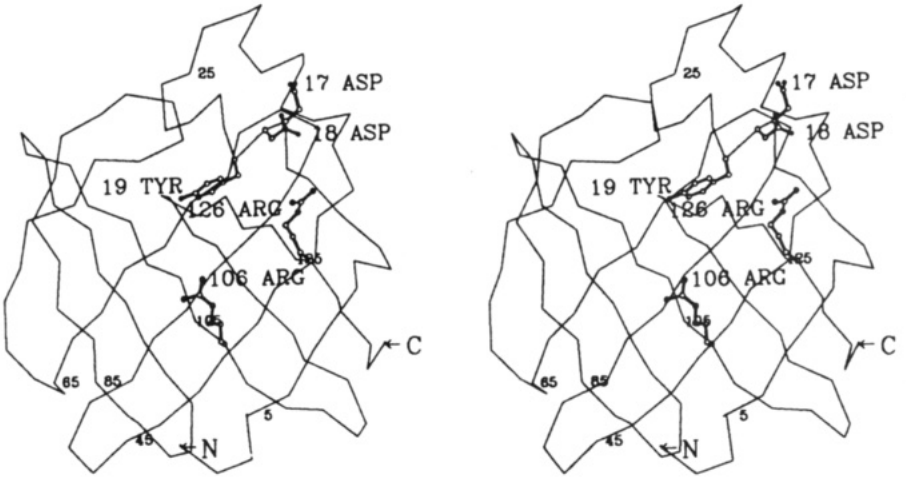

FIGURE 7: Stereodiagram of apo-ALBP. The stereodiagram represents the α-carbon model of apo-ALBP. Several side chains of interest are indicated, drawn in the form of ball-and-stick models. When viewed in stereo, Tyr^{19} can be seen pointing into the center of the molecule where the ligand-binding site is presumably found.

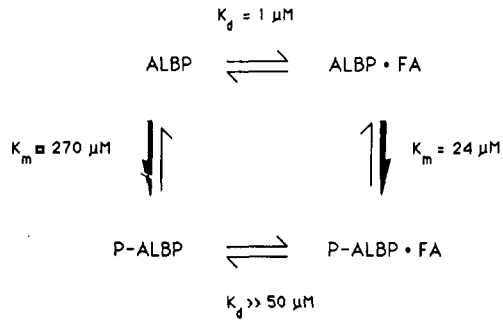

FIGURE 8: State diagram of phosphorylation and fatty acid binding of ALBP. ALBP·FA refers to the lipid binding protein/fatty acid complex. P-ALBP refers to the phosphorylated form of ALBP. All dissociation constants are apparent values determined using the 12-AO binding assay described under Experimental Procedures. The K_m values refer to the forward phosphorylation reaction (indicated by the bold arrows) using either apo- or holo-ALBP and the soluble kinase domain of the human insulin receptor [taken from Buelt et al. (1991)].

ALBP, it appears as though the primary reason is the limited accessibility of the kinase to the site of phosphorylation, Y19. The hydroxyl group of tyrosine lies approximately 10 Å from the protein surface, making direct kinase attack unlikely. We have studied the location of Tyr^{19} using computer graphics to see whether simple bond rotations can bring this side chain to the surface and therefore to a kinase-accessible position. It is clear that rotation around $\chi 1$ and $\chi 2$ of Tyr^{19} would create numerous unfavorable contacts with other elements of the protein and could only be achieved through significant main-chain conformational changes. Therefore, accessibility of the tyrosyl residue presumably results from a conformational alteration in the helix–turn–helix region which is generated by ligand binding and/or by kinase association.

The second structure/function question relates to the conformation of the protein after phosphorylation. Although ALBP appears to retain structural integrity upon phosphorylation (Figures 1 and 2), it exhibits a dramatically reduced affinity for fatty acid (Figures 4 and 5). One explanation for this reduction is that after modification, Tyr^{19} returns to its internal position as shown in Figures 6 and 7. Extrapolating from the crystal structure of apo-ALBP, one can predict that a phosphoryl moiety pointing into the binding cavity would hinder specific fatty acid association. However, the modified protein is quantitatively recognized by a monoclonal antibody to phosphotyrosine; this observation was exploited in order to isolate homogeneous phospho-ALBP. Furthermore, phospho-ALBP is readily dephosphorylated by two different tyrosyl phosphatases, human adipocyte acid phosphatase and GST-PTPU323 (Shekels et al., 1992). Taken together, these results suggest either that the phosphotyrosyl side chain is solvent accessible or that it becomes accessible in dynamical states. Alternatively, phosphorylated Tyr^{19} may lie in some intermediate position, blocking ligand exchange either sterically or due to its localized negative charge. We cannot rule out the possibility that local conformational changes occurred in the binding cavity that were not detected by our analyses.

The state diagram shown in Figure 8 summarizes the phosphorylation and fatty acid binding properties of the adipocyte lipid-binding protein. ALBP binds fatty acid with high affinity (K_d = 0.5–1 μM). Fatty acid binding presumably elicits some conformational change in ALBP which increases the affinity of the insulin receptor for the protein as demonstrated by a 10-fold reduction in K_m for phosphorylation (Buelt et al., 1991; Hresko et al., 1990). Phosphorylation inhibits ligand binding and, assuming a single entry/exit portal for the fatty acid, its release. The blocking of fatty acid exchange suggests that the protein must be dephosphorylated to allow for normal lipid trafficking. Its affinity for fatty acids makes ALBP an intriguing putative intermediate in insulin-stimulated processes such as glucose uptake and lipogenesis in the adipocyte, yet to date no clear function of the phosphorylated protein has been determined. Two hypotheses have been proposed (Hresko et al., 1990; Shekels et al., 1992) for the role of ALBP phosphorylation. The insulin-stimulated phosphorylation of holo-ALBP at the plasma membrane may serve to target the protein with its bound fatty acid to the microsomal membrane. A tyrosyl phosphatase on the membrane would dephosphorylate the protein, thus allowing the lipid to dissociate and undergo esterification. ALBP would then be capable of solubilizing other fatty acids for trafficking, thus creating an insulin-dependent cycling of fatty acids from the plasma membrane to the endoplasmic reticulum for utilization. This proposal is consistent with the in situ evidence presented by Waggoner and Bernlohr (1990) that ALBP plays a role in fatty acid uptake and trafficking. This model requires the involvement of a membrane-bound tyrosyl phosphatase specific for ALBP; two such phosphatases which are sensitive to PAO have been identified in 3T3-L1 adipocyte membranes by Liao et al. (1991).

A second hypothesis proposes that the turnover of phospho-ALBP is an intermediate step in the insulin signaling pathway (Hresko et al., 1988).[2] Phospho-ALBP itself then would play no fundamental function of its own other than as an intermediary. Our laboratory has isolated a soluble PAO-inactivated tyrosyl phosphatase from adipocytes and found it to be related to a family of low molecular weight phosphatases from placenta, heart, and liver (Zhang & Van Etten, 1990).[2] The bovine heart acid phosphatase exhibits marked phosphoryltransferase activity in vitro (Zhang & Van Etten, 1990). The adipocyte counterpart may function similarly, dephosphorylating phospho-ALBP and transferring the phosphoryl group to some acceptor molecule for propagation of the insulin signal. While the phosphoryltransferase hypothesis is intriguing, we favor the lipid trafficking hypothesis for it relates the lipid-binding capacity of the protein to the phosphorylation properties.

In summary, the results presented here characterizing the structural and ligand-binding properties of phospho-ALBP support the hypothesis that the protein is a physiological target of the insulin receptor kinase. This study, along with the crystal structure (Xu et al., 1992), provides insight into the basic structural principles for ALBP phosphorylation and function. Two hypotheses have been presented illustrating roles for phospho-ALBP function. The molecular details necessary to evaluate these proposals await further biochemical experimentation and determination of the crystal structures of holo- and phospho-ALBP.

ACKNOWLEDGMENTS

We thank Dr. L. Ellis (Dallas, TX) for generously providing the soluble kinase domain of the human insulin receptor and Dr. J. Dixon (Ann Arbor, MI) for the plasmid pKG-PTPU323. We also thank Drs. V. Matarese for preliminary fluoresence analysis and A. Bertazzon for assistance with circular dichroic analysis, as well as L. Shekels for many valuable discussions during the course of this work.

Registry No. Tyr, 60-18-4; lauric acid, 143-07-7; Sepharose 4B, 9012-36-6; oleic acid, 112-80-1.

REFERENCES

Baxa, C. A., Sha, R. S., Buelt, M. K., Smith, A. J., Matarese, V., Chinander, L. L., Boundy, K. L., & Bernlohr, D. A.

(1989) *Biochemistry 28*, 8683–8690.
Bernier, M., Laird, D. M., & Lane, M. D. (1987) *Proc. Natl. Acad. Sci. U.S.A. 84*, 1844–1848.
Bernier, M., Laird, D. M., & Lane, M. D. (1988) *J. Biol. Chem. 263*, 13626–13634.
Bernlohr, D. A., Bolanowski, M. A., Kelly, T. J., & Lane, M. D. (1985) *J. Biol. Chem. 260*, 5563–5567.
Buelt, M. K., & Bernlohr, D. A. (1990) *Biochemistry 29*, 7408–7413.
Buelt, M. K., Shekels, L. L., Jarvis, B. W., & Bernlohr, D. A. (1991) *J. Biol. Chem. 266*, 12266–12271.
Chang, C. T., Wu, C.-S., & Yang, J. T. (1978) *Anal. Biochem. 91*, 13–31.
Chinander, L. L., & Bernlohr, D. A. (1989) *J. Biol. Chem. 264*, 19564–19572.
Cistola, D. P., Walsh, M. T., Corey, R. P., Hamilton, J. A., & Brecher, P. (1988) *Biochemistry 27*, 711–717.
Cobb, M. H., Sang, B.-C., Gonzalez, R., Goldsmith, E., & Ellis, L. (1989) *J. Biol. Chem. 264*, 18701–18706.
Cooper, J. A., Esch, F. S., Taylor, S. S., & Hunter, T. (1984) *J. Biol. Chem. 259*, 7835–7841.
Ellis, L., Clauser, E., Morgan, D. O., Edery, M., Roth, R. A., & Rutter, W. J. (1986) *Cell 45*, 721–732.
Endemann, G., Yonezawa, K., & Roth, R. A. (1990) *J. Biol. Chem. 265*, 396–400.
Escobedo, J. A., Navankasattusas, S., Kavanaugh, W. M., Milfay, D., Fried, V. A., & Williams, L. T. (1991) *Cell 65*, 75–82.
Guan, K., & Dixon, J. E. (1991) *Anal. Biochem. 192*, 262–267.
Guan, K., Haun, R. S., Watson, S. J., Geahlen, R. L., & Dixon, J. E. (1990) *Proc. Natl. Acad. Sci. U.S.A. 87*, 1501–1505.
Herrera, R., Lebwohl, D., de Herreros, A. G., Kallen, R. G., & Rosen, O. M. (1988) *J. Biol. Chem. 263*, 5560–5568.
Hresko, R. C., Bernier, M., Hoffman, R. D., Flores-Riveros, J. R., Liao, K., Laird, D. M., & Lane, M. D. (1988) *Proc. Natl. Acad. Sci. U.S.A. 85*, 8835–8839.
Hresko, R. C., Hoffman, R. D., Flores-Riveros, J. R., & Lane, M. D. (1990) *J. Biol. Chem. 265*, 21075–21085.
Hunt, C. R., Ro, J. H.-S., Dobson, D. E., Min, H. Y., & Spiegelman, B. M. (1986) *Proc. Natl. Acad. Sci. U.S.A 83*, 3786–3790.
Jones, T. A., Bergfors, T., Sedzik, J., & Unge, T. (1988) *EMBO J. 7*, 1597–1604.
Kabsch, W., & Sander, C. (1983) *Biopolymers 22*, 2577–2637.
Koch, C. A., Anderson, D., Moran, M. F., Ellis, C., & Pawson, T. (1991) *Science 252*, 668–674.
Kohanski, R. A., & Lane, M. D. (1983) *J. Biol. Chem. 258*, 7460–7468.
Liao, K., Hoffman, R. D., & Lane, M. D. (1991) *J. Biol. Chem. 266*, 6544–6553.
Matarese, V., & Bernlohr, D. A. (1988) *J. Biol. Chem. 263*, 14544–14551.
Matarese, V., Stone, R. L., Waggoner, D. W., & Bernlohr, D. A. (1990) *Prog. Lipid Res. 28*, 245–272.
Morgan, D. O., & Roth, R. A. (1987) *Proc. Natl. Acad. Sci. U.S.A. 84*, 41–45.
Nagy, B., & Strzelecka-Golaszewska, H. (1972) *Arch. Biochem. Biophys. 150*, 428–435.
Ray, L. B., & Sturgill, T. W. (1988) *Proc. Natl. Acad. Sci. U.S.A. 85*, 3753–3757.
Ropson, I. J., Gordon, J. I., & Frieden, C. (1990) *Biochemistry 29*, 9591–9599.
Rosen, O. M. (1987) *Science 237*, 1452–1458.
Ruderman, W. B., Kapellar, R., White, M. F., & Cantley, L. C. (1990) *Proc. Natl. Acad. Sci. U.S.A. 86*, 1411–1415.
Sacchettini, J. C., Gordon, J. I., & Banaszak, L. J. (1989a) *J. Mol. Biol. 208*, 327–339.
Sacchettini, J. C., Gordon, J. I., & Banaszak, L. J. (1989b) *Proc. Natl. Acad. Sci. U.S.A. 86*, 7736–7740.
Sadowski, I., Stone, J. C., & Pawson, T. (1986) *Mol. Cell Biol. 6*, 4396–4408.
Shekels, L. L., Smith, A. J., Van Etten, R. L., & Bernlohr, D. A. (1992) *Protein Sci.* (in press).
Shortle, D. (1989) *J. Biol. Chem. 264*, 5315–5318.
Storch, J., Bass, N. M., & Kleinfeld, A. M. (1989) *J. Biol. Chem. 264*, 8708–8713.
Sweetser, D. A., Heuckeroth, R. O., & Gordon, J. I. (1987) *Annu. Rev. Nutr. 7*, 337–359.
Waggoner, D., & Bernlohr, D. A. (1990) *J. Biol. Chem. 265*, 11417–11420.
White, M. F., & Kahn, C. R. (1986) *The Enzymes 17*, 247–310.
White, M. F., Maron, R., & Kahn, C. R. (1985) *Nature 318*, 183–186.
Xu, Z., Bernlohr, D. A., & Banaszak, L. J. (1992) *Biochemistry* (preceding paper in this issue).
Xu, Z., Buelt, M. K., Banaszak, L. J., & Bernlohr, D. A. (1991) *J. Biol. Chem. 266*, 14367–14370.
Zhang, Z.-Y., & Van Etten, R. L. (1990) *Arch. Biochem. Biophys. 282*, 39–49.